Sensitivity measurement of a cantilever-based surface stress sensor

Ann-Lauriene Haag,[a] Zeno Schumacher, and Peter Grutter
Department of Physics, Ernest Rutherford Physics Building, McGill University, 3600 Rue University, Montreal, Quebec H3A 2T8, Canada

(Received 8 August 2016; accepted 4 October 2016; published online 19 October 2016)

A detailed analysis of the temporal surface stress evolution for potential-driven adsorption of ions is discussed. A gold-coated cantilever is used to simultaneously measure the change in surface stress as well as the current response during an applied potential step. In this electrochemical configuration, the cantilever acts as the working electrode, a platinum wire as the counter electrode, and the Ag/AgCl (sat. KCl) electrode as the reference electrode. To study the time-dependent signal and the sensitivity of the cantilever response, the frequency of the potential step applied to the cantilever is varied from 1 s to 0.1 ms. First, a comparison between a strong adsorbing (chloride Cl^-) and a weak adsorbing ion (perchlorate ClO_4^-) in a 1 mM solution is presented. Next, the linear relationship between surface stress and charge density is measured for these fast potential steps. The slope of this fit is defined as the sensitivity of the system and is shown to increase for shorter potential pulses. Finally, the behaviour of the surface stress and current for consecutive applied potential steps is studied. *Published by AIP Publishing.* [http://dx.doi.org/10.1063/1.4964922]

I. INTRODUCTION

In recent years, several nano and micromechanical structures have been described as possible biosensor platforms.[1–5] Here we focus on cantilever-based sensors which have been used for the mechanical detection of a vast variety of biological targets such as DNA,[6–15] antigens,[16] proteins,[17,18] bacteria,[19–21] and viruses.[22] The most common detection principles in these mechanical sensors due to biological binding effects are changes in surface stress[23–27] and mass.[28–31] For the sensing of oligonucleotides under potential-control, we have shown that the ion adsorption dominates the magnitude of the surface stress signal.[12] An important consequence of this is that the magnitude of the observed stress signal is proportional to the area of exposed clean gold.[8] In this study, a gold-coated cantilever sensor is used to measure surface stress changes upon exposure to a 1 mM NaCl or $NaClO_4$ solution under potential control. A three-electrode electrochemical system, with the cantilever connected as the working electrode, is used to apply potentials to the surface of the cantilever. Ions are directed to the surface and these accumulated charges cause a substantially larger measurable change in the surface stress[8,12,24] over conventional surface stress measurements at open-circuit potentials.

In this paper, we apply a series of potential steps to the gold-coated cantilever surface with decreasing pulse width and the resulting surface stress change as well as the current response is simultaneously measured. The current can be integrated and normalized by the sensors area to determine the charge density and correlate it with the stress response.

It has been shown that the surface stress change is linearly related to the surface charge density for Au(111) for different ion species[32–34] with a characteristic proportionality coefficient ξ defined by the slope of the plot of surface stress σ versus charge density q,

$$\xi = \frac{d\sigma}{dq}. \tag{1}$$

The coefficient is a measure of the stress sensitivity of the cantilever sensor. A larger value corresponds to a larger slope which means that a small change in charge density corresponds to a large change in surface stress. Several studies have analyzed this coefficient on metal electrodes. In particular, Haiss *et al.*[32] used a flame-annealed gold-coated glass cantilever and Ibach *et al.*[34] used a macroscopic Au(111) single crystal cantilever to measure this parameter. Both studies measured the potential-induced deflection of the cantilever using Scanning Tunneling Microscopy (STM). Tabard-Cossa *et al.* have shown the stress-charge relationship on a polycrystalline Au(111) microcantilever.[33] All measurements observed a negative surface stress–charge coefficient with reported ξ-values between −0.67 V and −2.0 V for chloride adsorption.[32,33,35–41] Several factors play a role in the variation of these values. These include but are not limited to cleanliness of the surface and surface treatment,[33] different crystal orientation (single-crystal vs. polycrystalline),[36] investigated potential window,[39] ion concentration,[42] and measurement method. As pointed out in a recent study, the surface roughness of the metal electrode can change the coefficient value from −0.7 V (for rough surfaces) to −1.15 V (for smooth surfaces).[41] None of these studies have investigated the temporal evolution of the coefficient and only operate in steady-state conditions. We show, for the first time, the behavior of the coefficient ξ on a gold-coated cantilever on decreasing potential step width in a 1 mM NaCl and 1 mM $NaClO_4$ solution.

A. Fast-potential pulses

To measure the time-resolved surface stress and current signals, the length of the applied potential pulse is decreased.

[a]Electronic mail: haagal@physics.mcgill.ca

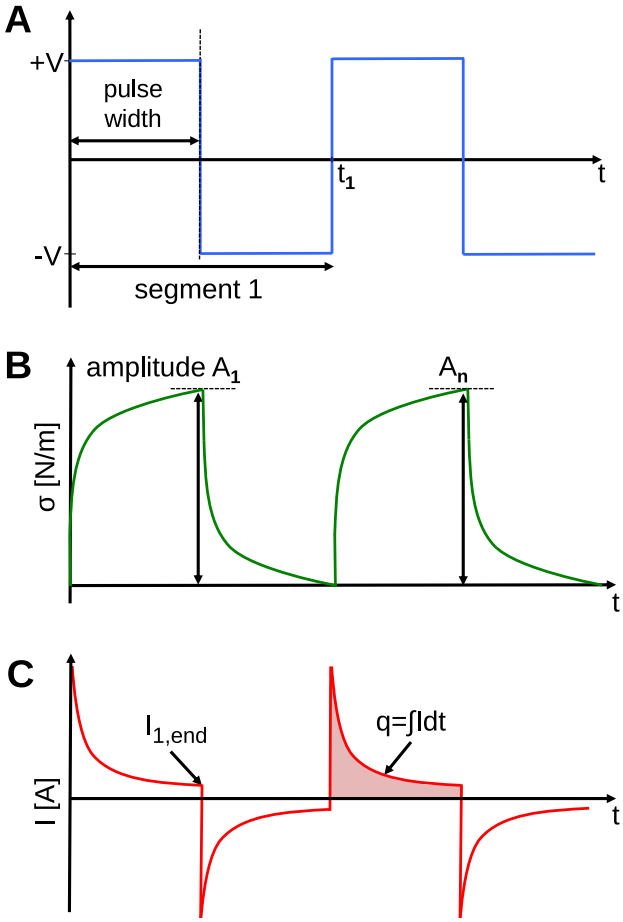

FIG. 1. Schematics for fast potential switch measurement, showing the input voltage (a), the surface stress response (b) and the current recording (c).

A potential pulse between ±0.1 V and 0.5 V with a defined pulse width (ranging from 1 s to 0.1 ms) is applied to the gold-coated cantilever for 5 segments (Figure 1(a)). The potential values are chosen so that no redox reaction in the solution or the gold occurs. The shortest pulse width (0.1 ms) is limited by the potentiostat setting used for these experiments (CHI 1030A, CH Instruments, USA). The cantilever is exposed to either 1 mM sodium chloride (NaCl) or 1 mM sodium perchlorate ($NaClO_4$) solution after an electrochemical cleaning.[8] Chloride and perchlorate ions will induce a change in the surface stress of the cantilever which can be monitored using standard beam deflection methods. A fast change in the surface stress followed by a slower change is observed until equilibrium is reached and schematically shown in Figure 1(b). The first rise is correlated with the well-known double layer charging of the interface as observed in the current data. The slower change correlates to the diffusion of ions towards the surface until the electrode surface is screened and equilibrium conditions are established. The characteristic surface stress change amplitude A_n for each segment is defined as the distance between the last value of the first segment and the last value of the second segment. With the three-electrode configuration, the current vs. time response can be simultaneously measured (Figure 1(c)). A sharp current spike is first observed followed by a slower current decay until equilibrium conditions are reached. The sharp spike comes from the instantaneous change in potential and the subsequent instant drive of ions to the surface and has a time constant in the order of 10 μs for an applied potential of 100 mV in a 1 mM solution.[43] More ions will then diffuse towards the electrode to form a complete double-layer. The potential here is low enough to inhibit electrochemical reactions (i.e., redox reactions); therefore, the current will fall back to zero after the double layer is formed and equilibrium conditions are established. The presence of faradaic processes (e.g., reduction/oxidation of gold) would lead to a constant current flow and the recorded current will not go back to zero. By decreasing the time of the applied potential pulse, larger I_{end} current values are recorded because equilibrium conditions are not yet established. The recorded current can be integrated over time (and divided by the electrochemical area of the cantilever) to yield the charge density profile. The electrochemical area is determined by integrating the gold reduction peak of a cyclic voltammetry recorded in 50 mM $KClO_4$ and dividing this by the standard gold charge.[44]

By varying the pulse width t_1, the change between equilibrium and transient conditions is monitored. The potential-dependent conditions are further studied by varying the applied potential between 0.1 V and 0.5 V. The surface stress increases with increased applied surface potential, as more ions are directed to the surface inducing a larger surface stress signal.

If a potential step is applied to a system in the solution, the current response is described by the Cottrell equation.[45] However, the Cottrell equation only describes the faradaic current which is observed after the initial double layer contribution. The initial current response is dominated by the charging current for the double layer formation and is expressed by

$$i_{ch} = \frac{\Delta E}{R_s} exp\left(-\frac{t}{R_s C_d}\right), \tag{2}$$

with ΔE the potential step, R_s the serial resistance, and C_d the double layer capacitance. The double layer capacitance C_d is described by the Gouy-Chapman-Stern model and is dependent on several parameters including the ion concentration ρ_0 and the electric potential ϕ. Both of these parameters are time-dependent and change over the course of the applied potential step. Therefore, this equation can only be solved numerically. Only recently have results been reported for saline solutions[43] and pure water.[46] For small gaps defined by $A \gg d^2$, Marrow-Sato[47] derived the following equation so that the current, I, that is flowing due to an applied potential in a sodium chloride solution is described by:

$$I = \frac{A}{d}\left(e\int_0^d \left[\rho_{Na^+}W_{Na^+} - \rho_{Cl^-}W_{Cl^-} + D_{Na^+}\frac{\partial \rho_{Na^+}}{\partial x} - D_{Cl^-}\frac{\partial \rho_{Cl^-}}{\partial x}\right]dx + \epsilon_r\epsilon_0\frac{\partial E}{\partial t}\right), \tag{3}$$

which is dependent on the ion number density for sodium ions and chloride ions (ρ_{Na^+} and ρ_{Cl^-}), the ion drift velocities (W_{Na^+} and W_{Cl^-}), and the diffusion coefficients (D_{Na^+} and D_{Cl^-}). The ion drift velocity is the flow velocity that the ion has due to the applied potential field. This equation will result in the true total current flowing due to an applied voltage step.

In our experimental setup, the simplified Morrow-Sato form shown in Equation (3) is not valid, as small gaps are not present. The size of the electrode is much smaller than the distance between electrodes (in the order of cm). Therefore, it is not trivial to quantitatively describe the current response without numerically solving the equation. In this paper, an experimental description of the current response due to short applied potentials is shown for chloride and perchlorate ions and correlated with surface stress measurements.

II. MATERIALS AND METHODS

A. Gold surface preparation

Measurements were performed on a tipless silicon cantilever (CSC38, MikroMash, USA). The cantilevers were solvent cleaned (acetone, ethanol, isopropanol) before thermal evaporation of an adhesion layer of 2 nm titanium followed by 100 nm of gold under ultra-high vacuum conditions. Evaporation rates for titanium were set to 0.9 Å/s and 1 Å/s for gold (pressure $<1 \times 10^{-6}$ mbar, room temperature). Samples were stored under ambient conditions until needed. To define the electrochemically active area of the exposed gold in solution, a thin layer of Eccobond 286 (Emerson & Cuming, USA) was applied to the base of the gold-coated cantilever leaving a defined exposed area.

B. Solutions

All salts were purchased from Sigma-Aldrich (USA) and were prepared using Mili-Q water. NaCl and $NaClO_4$ concentrations were set to 1 mM so that a reasonable large diffuse layer thickness (9.62 nm based on the Gouy-Chapman model) and slow measureable time scales were achieved. Increasing these concentrations leads to short diffuse layers and a faster dynamic which is more challenging to measure. However, we believe that changing the salt concentration will result in qualitatively similar results.

C. Electrochemical control

All electrochemical measurements were performed in a three-electrode configuration, with a platinum wire as the counter electrode (1 mm diameter, Alfa Aesar, USA), the cantilever as the working electrode, and an Ag/AgCl (sat. KCl) reference electrode (BASi, USA) as the reference. The electrochemical control was done using a CHI 1030A (CH Instruments, USA) potentiostat. Prior to each experiment, the cantilevers were electrochemically cleaned by cycling the potential from −0.8 V to 1.4 V vs. Ag/AgCl (sat. KCl) in 50 mM $KClO_4$ at a scan rate of 20 mV/s until a reproducible signal was observed. Potential steps rather than sweeps were applied to the working electrode so that the instant change of the surface stress and the current was measured.

D. Current measurement

The current response was measured using the CHI 1030A (CH Instruments, USA) potentiostat. A step potential was applied to the working electrode in solution and the resulting current response was recorded. The sampling rate was set to 50 000 samples/s and the potential width was set to 1 s, 0.1 s, 0.01 s, and 0.001 s. The 0.001 s pulse was the lowest setting to measure reasonable surface stress changes. Applied potential pulses varied from ±0.1 to 0.5 V to measure a wide range of potential windows. No redox reactions were observed for the given potential range.

E. Surface stress measurement

After the electrochemical cleaning step, cantilevers were immersed into a 1 mM solution of either sodium chloride (NaCl) or sodium perchlorate ($NaClO_4$). Five potential pulses (segments) between ±0.1 V and 0.5 V were applied to the cantilever. The potential pulses were varied from 1 s to 0.1 ms. Surface stress changes were measured by standard beam-deflection methods. A laser was aligned to the cantilever so that a change in bending due to an applied potential was measured with a position sensitive diode (PSD). By using Stoney's formula,[48] the measured change in the voltage of the photodiode can be converted into a surface stress change.

III. RESULTS AND DISCUSSION

A. Weak versus strong adsorbing ions

Current and surface stress measurements were done on a gold-coated cantilever in two different solutions: 1 mM $NaClO_4$ and 1 mM NaCl. The latter one contains strongly adsorbing chloride ions and the first one more weakly adsorbing perchlorate ions. Chloride, like other halides, is a quasi-spherical anion with its negative charge well distributed. It can therefore easily share its negative charge with an empty d-orbital from the gold surface to form a dipole. Perchlorate ions, however, have their negative charge not well distributed because only one of the four oxygens is negatively charged. Interactions with gold are therefore less efficient. Chloride ions have an ionic radius (including the hydration shell) of 167 pm, whereas perchlorate ions are roughly twice as large at 309 pm.[49] This means fewer perchlorate ions can interact with the surface per unit area and that each perchlorate ion interacts weaker with the gold surface than a chloride ion.

For all measurements, 5 potential pulses between ±0.2 V (vs. Ag/AgCl (sat. KCl)) are applied to the cantilever in a three-electrode configuration. The pulse width is then decreased from 0.5 s to 0.001 s. All current values are converted into the current density by dividing the current with the electrochemical surface area of the electrode. In Figure 2, the current response for all pulse widths are shown. For better clarity, all segments are stretched in the x-direction, so that the length of the pulse is the same. Clearly, the

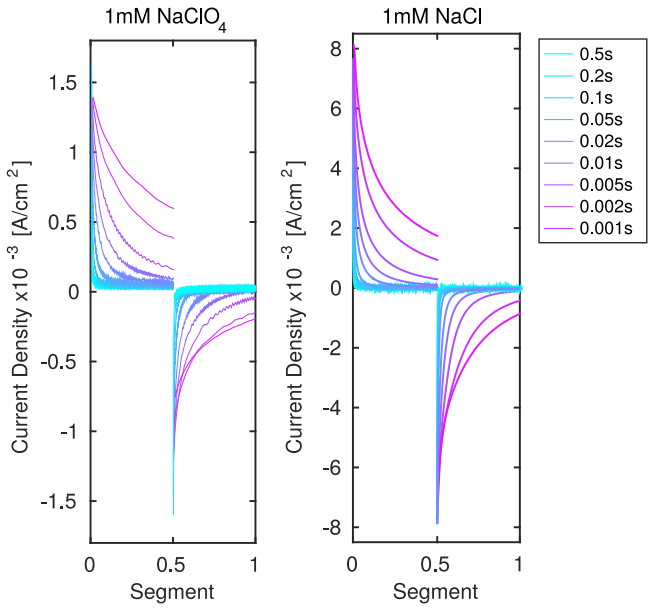

FIG. 2. Current response for 1 mM $NaClO_4$ and NaCl for a potential pulse at ±0.2 V (vs. Ag/AgCl (sat. KCl)). The current is plotted against the segment meaning that each pulse width is stretched. The pulse width is varied from 0.5 s (light blue) to 0.001 s (pink). The x-axis is normalized to the segment length. Note the difference in the current axis for both plots.

maximum peak current value is smaller for $NaClO_4$ than for NaCl, 1.5×10^{-3} A/cm^2 and 8×10^{-3} A/cm^2, respectively. For longer pulse width, the current decays to values close to zero (light blue traces). However, for potential pulses shorter than 0.05 s current values higher than zero are measured. This is because the potential is switched before the current reaches equilibrium. This behavior is observed for both solutions.

The corresponding surface stress response for both solutions is shown in Figure 3. Results for $NaClO_4$ show a maximum surface stress change amplitude of 35 mN/m for the longest pulse (0.5 s, light blue). This surface stress amplitude reduces to less than 7 mN/m for the shortest measured pulse (0.001 s, pink). As expected, for NaCl the surface stress change is larger and decreases from 120 mN/m to 18 mN/m. A roughly 3.5-times increase in the surface stress is observed for the more strongly adsorbing chloride ions corresponding to a similar increase in the current peak (Figure 2). Clearly, to achieve a large surface stress signal in potential-driven measurements a chloride-containing solution is the preferred choice.[8]

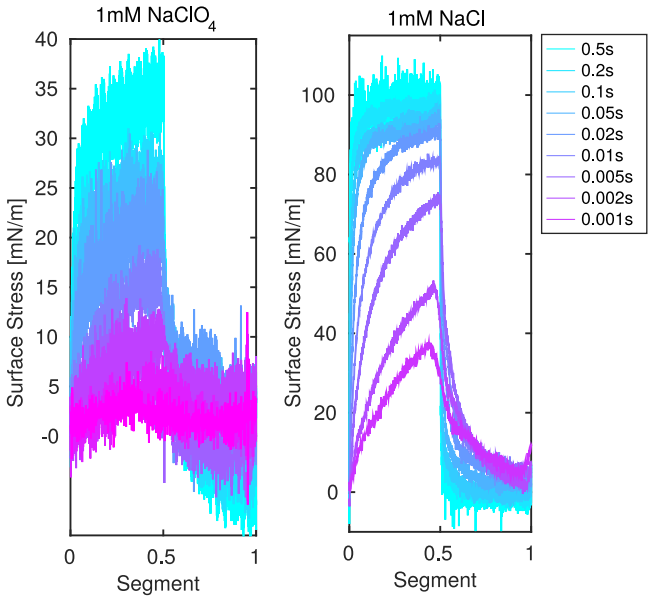

FIG. 3. Surface stress response for 1 mM $NaClO_4$ and NaCl for a potential pulse at ±0.2 V (vs. Ag/AgCl (sat. KCl)) with a width of 0.5 s (light blue) to 0.001 s (pink). The x-axis is normalized to the segment length.

In the following, we will investigate the response for consecutive segments giving insights into the dynamics of the system.

B. Coefficient ξ at decreasing pulse width

Potential pulses from 0.1 V to 0.5 V are applied to the gold-coated cantilever electrode. The potential width is decreased from 1 s to 0.1 s, 0.01 s, and 0.001 s and the resulting surface stress and charge density are simultaneously recorded. The coefficient values ξ for the cantilever response for decreasing potential pulses in 1 mM NaCl are shown in Figure 4. The surface stress against the charge density plot for one potential width is shown Figure 4(b). The error bars for each voltage step are the standard deviation for five independently performed experiments on different cantilevers. It is assumed that at zero charge density, no surface stress is observed, therefore, no y-offset is applied.

An increase in the coefficient is seen for shorter pulses, from $\xi = 0.44$ V ± 0.02 V for 1 s pulses to $\xi = 0.74$ V ± 0.02 V for 0.001 s pulses. Recall that a larger coefficient means that a small change in charge results in a higher change of the surface stress signal, indicating that the stress sensing is more sensitive to changes in charge for shorter pulses.

For shorter pulses, the initial double layer charging is measured, which happens on a faster time scale. For pulses at 0.001 s, only the first charges contribute to the cantilever stress measurement. As observed in Figure 2, the current shows a more rapid decay at the beginning followed by a slower response until the system reaches equilibrium. Therefore, for longer pulses, the additional diffusion of ions towards the surface plays an important role and leads to an overall reduction of stress signal. In summary, the surface stress–charge coefficient ξ tracks the changes of the surface stress sensitivity of the system. A larger coefficient ξ value is observed for shorter potential steps, indicating that the surface stress is more sensitive towards the initial charge transfer (i.e., double layer formation) than towards the bulk diffusion happening on a longer time scale. The ξ value therefore allows us to track the sensitivity of the system as well as the different phenomena contributing to the overall surface stress signal. Clearly, the ions forming the double layer (i.e., the charges close to the surface) lead to a larger surface stress then those that diffuse slower and are further away from the surface. By performing time resolved stress sensing, one is thus effectively performing a measurement of the location of ions with respect to the cantilever. This is of relevant if one wants to qualitatively and quantitatively understand

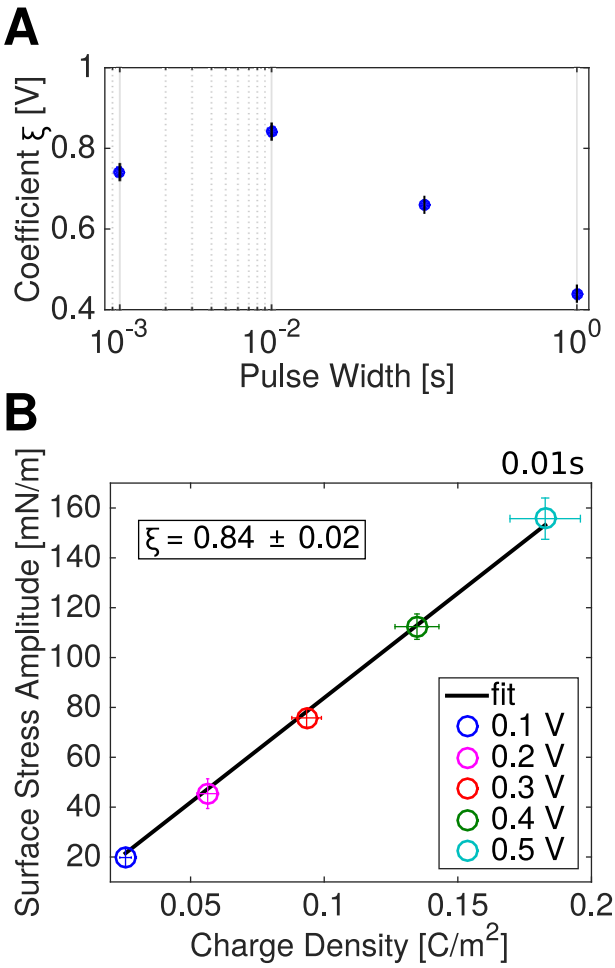

FIG. 4. (a) Surface stress change–charge coefficient for decreasing potential pulses (1, 0.1 s, 0.01 s, and 0.001 s) at potentials between 0.1 V and 0.5 V (vs. Ag/AgCl (sat. KCl)) in 1 mM NaCl. (b) The potential-dependent surface stress and charge density mean and standard deviation for five different cantilevers at 0.01 s are plotted.

stress signals observed for complex systems such as DNA in solution.[8,12]

C. Segment-specific behavior

The magnitude of the ξ coefficient evolves for consecutively measured segments. The correlation coefficient is plotted for segments 1-5 for a pulse width of 0.001 s (Figure 5) in 1 mM NaCl at potentials between ±0.1 V and ±0.5 V (vs. Ag/AgCl (sat. KCl)). The error bars are from the fitting of the experimental data.

We observe that the coefficient ξ increases with the segment number, from $\xi = 0.49\ \text{V} \pm 0.06\ \text{V}$ for the first segment to $\xi = 0.96\ \text{V} \pm 0.17\ \text{V}$ for the fifth segment for potential pulses at 0.001 s. This increase can be explained by the extra charge accumulation for each segment at these short pulse widths. The current response does not allow a complete double layer to be built by the time the potential switches. Therefore, extra chloride ions will be transferred to the next segment. This increases the local concentration of chloride ions and less chloride from the bulk is needed for the new double layer build-up.

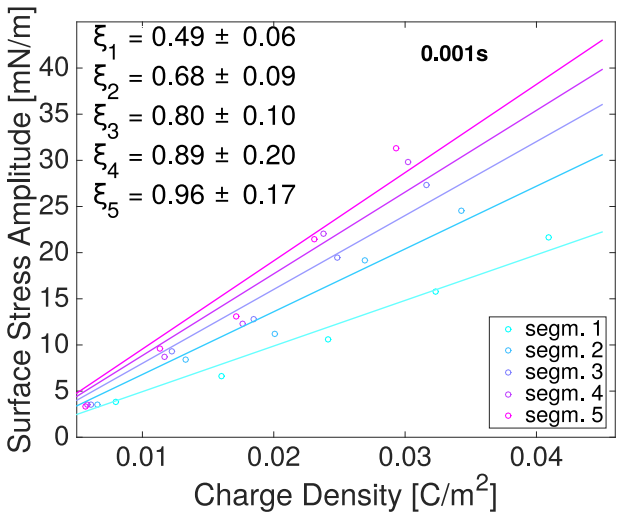

FIG. 5. Surface stress change–charge coefficient for each of the five positive potential segments for a 0.001 s potential pulse.

We thus interpret that the first segment probes a thicker doubler layer than the last segment. The double layer thickness is defined by the Debye length κ^{-1} as

$$\kappa^{-1} = \sqrt{\frac{\epsilon\epsilon_0 k_B T}{2e^2\rho_0}}, \tag{4}$$

with ρ_0 the ion concentration, ϵ the dielectric constant of the medium, and ϵ_0 the vacuum permittivity. The Debye length quantitatively describes the thickness of the diffuse layer and therefore how far into the solution a surface potential reaches. The Debye length in a 1 mM sodium chloride concentration is 96 Å. If the local concentration ρ_0 is increased for each segment, the established Double layer thickness will be decreased. This is in line with the results shown in Figure 5, where higher sensitivities are reached for shorter pulses as this probes a thinner layer.

To take a different look at this behavior, the results for two different potential pulse widths (0.1 s and 0.001 s) for a potential at ±0.4 V (vs. Ag/AgCl (sat.KCl)) are investigated for all segments. In Figure 6, the surface stress versus charge density plot for 1 mM NaCl (red) and 1 mM $NaClO_4$ (blue) is shown. The direction of the data within the segments is highlighted by an arrow pointing from the first to the fifth segment. The signal changes most prominently between the first and the second segment and then rapidly seems to reach a steady-state value.

It is expected that an increase in the charge density results in an increase of the surface stress change. However, this is only observed for NaCl at longer potential pulses. In contrast, for $NaClO_4$ and for short potential pulses (0.001 s), a decrease in charge density and an increase in surface stress is observed for consecutive segments at the same potential. This can be explained by the fact that for short pulses, the system does not obey equilibrium conditions anymore and an incomplete double layer is built up. This is in agreement with the observations in Figure 5.

We assume that the increase in concentration changes the starting conditions of the pulse and therefore fewer ions are

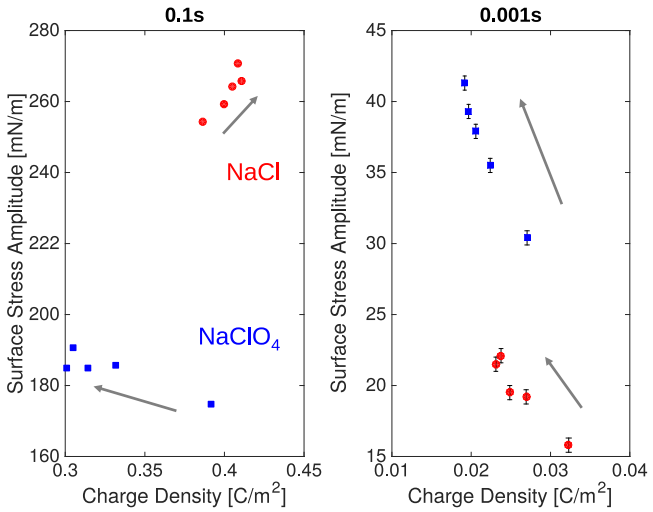

FIG. 6. Surface stress change amplitude of the cantilever versus the charge density measured from the current response for 1 mM NaCl (red) and 1 mM $NaClO_4$ (blue) at a potential width of 0.1 s and 0.001 s pulses at 0.4 V.

needed to build up the double layer for the next segment, since the debye length is inversely proportional to the ion concentration. This leads to a decrease of current flow and thus charge density as observed in Figure 6. The additional chloride ions add to the initial concentration, leading to higher concentration values for increasing segments. Furthermore, the increase of concentration near the surface leads to an increase in surface stress change. Therefore, for shorter potentials (<0.1 s), the charge is inversely dependent on the surface stress ($q \propto 1/\sigma$) within consecutive segments. The ξ value for different potential still follows the linear dependence described above. The effect within the segments is, however, dependent on the diffusion coefficient of the anion being probed. If the potential pulse is slow enough so that equilibrium conditions are met, a linear dependence between surface stress and charge is observed. This is the case for the chloride ions at longer potential pulses (0.1 s). However, the inversely proportional effect is observed for perchlorate ions, as the diffusion time for these ions is longer (1.79×10^{-9} m^2/s for $ClO4^-$ and 2.03×10^{-9} m^2/s for Cl^-).[50]

IV. SUMMARY AND CONCLUSION

In summary, the time-dependent evolution of the surface stress and current signal of a gold-coated cantilever in a 1 mM NaCl and $NaClO_4$ solution is observed. Potential values between ±0.1 V and ±0.5 V (vs. Ag/AgCl (sat. KCl)) with decreasing potential width from 0.1 s to 0.1 ms are applied to the gold-coated cantilever electrode. Larger surface stress and current values are recorded for the stronger adsorbing chloride anion than for the weaker adsorbing perchlorate. By comparing the charge density with the surface stress, a linear relationship is found which is in agreement with previous studies.[32,33,35] Decreasing the potential pulse to 0.001 s results in an increase of the surface stress-charge coefficient ξ. A shorter pulse results in an incomplete double layer and therefore a thinner charge layer is probed. The coefficient is a measure of the sensitivity of the sensor, therefore, we conclude that for shorter pulses, a higher sensitivity is observed. The charge from this result in a higher change of surface stress than the compensating charge coming from the bulk diffusion being measured for longer pulses.

By analyzing the coefficient response for consecutively applied segments, a variation is observed. For 0.001 s, the coefficient for the first segment is smaller than for the consecutive segments (0.49 ± 0.06 Nm/C for the first and 0.96 ± 0.17 Nm/C for the last segment). The coefficient reaches a steady state after more than five segments in the case of 0.001 s. The local ion concentration increases due to the non-equilibrium conditions leading to a decrease in the diffuse layer length and therefore an increase in sensitivity. This is in agreement with the previously found increased sensitivity when a thinner layer is probed (faster potential pulses).

Finally, it is shown that for fast pulses, the charge density appears to be inversely proportional to the surface stress change within consecutive segments. As observed, the charge density decreases for increasing segments. This is assumed to be due to the extra chloride ions being transferred into the next segment. The extra ions increase the local concentration near the electrode and the charging current needs to be smaller, as less charge is needed to screen the electrode surface. This leads to a decrease in charge density with increasing segments. On the other hand, the increase in concentration leads to a smaller Debye length. We found that higher sensitivities and a larger absolute surface stress due to the increased concentration are measured.

As discussed above, quantitatively describing this system is not trivial, as all parameters are time-dependent. However, by numerically solving the particular current response for these fast switching potentials, one can extract the changes in ion concentration for each segment, as well as the resulting change in the probed diffuse layer thickness. This calculation will help to further utilize this concept for biosensing applications. The charge response of a biomolecule attached to the cantilever surface can be probed by reducing the applied pulse width and thus reducing the probed diffuse length. It has been demonstrated that charges along an antigen can be probed by changing the concentration of the probing solution.[51] A local change in concentration can be achieved with fast potentials or in observing the response as a function of the segment number, as outlined above. Consecutively applied potentials could, therefore, measure the contribution of the charge and surface stress change along a molecule. The advantage of this method is that experiments can be performed very fast (within minutes) and are label-free. The biomolecules do not need to be labeled with, e.g., a fluorescence molecule.

ACKNOWLEDGMENTS

This work was supported by the Natural Sciences and Engineering Research Council of Canada (NSERC) and the Regroupement quebecois sur les materiaux de pointe (RQMP). All authors thank Antonella Badia for her feedback on the manuscript. Ann-Lauriene Haag and Zeno Schumacher thank the Swiss National Science Foundation (SNF) for a DOC.Mobility Fellowship.

[1]J. Arlett, E. B. Myers, and M. L. Roukes, Nat. Nanotechnol. **6**, 203 (2011).
[2]T. Michels and I. W. Rangelow, Microelectron. Eng. **126**, 191 (2014).
[3]S. Mehrabani, A. Maker, and A. Armani, Sensors **14**, 5890 (2014).
[4]J. Tamayo, P. M. Kosaka, J. J. Ruz, Á. San Paulo, and M. Calleja, Chem. Soc. Rev. **42**, 1287 (2013).
[5]P. S. Waggoner and H. G. Craighead, Lab Chip **7**, 1238 (2007).
[6]R. Marie, H. Jensenius, J. Thaysen, C. B. Christensen, and A. Boisen, Ultramicroscopy **91**, 29 (2002).
[7]H. Hou, X. Bai, C. Xing, B. Lu, J. Hao, X. Ke, N. Gu, B. Zhang, and J. Tang, Talanta **109**, 173 (2013).
[8]A.-L. Haag, Y. Nagai, R. B. Lennox, and P. Grütter, EPJ Tech. Instrum. **2**, 1 (2015).
[9]J. C. Stachowiak, M. Yue, K. Castelino, A. Chakraborty, and A. Majumdar, Langmuir **22**, 263 (2006).
[10]K. Hansen, H. Ji, G. Wu, R. Datar, R. Cote, A. Majumdar, and T. Thundat, Anal. Chem. **73**, 1567 (2001).
[11]M. Álvarez, L. G. Carrascosa, M. Moreno, A. Calle, Á. Zaballos, L. M. Lechuga, C. Martínez-A, and J. Tamayo, Langmuir **20**, 9663 (2004).
[12]Y. Nagai, J. D. Carbajal, J. H. White, R. Sladek, P. Grutter, and R. B. Lennox, Langmuir **29**, 9951 (2013).
[13]A. Sassolas, B. D. Leca-Bouvier, and L. J. Blum, Chem. Rev. **108**, 109 (2008).
[14]J. Mertens, C. Rogero, M. Calleja, D. Ramos, J. A. Martín-Gago, C. Briones, and J. Tamayo, Nat. Nanotechnol. **3**, 301 (2008).
[15]D. Li, S. Song, and C. Fan, Acc. Chem. Res. **43**, 631 (2010).
[16]J. H. Lee, K. S. Hwang, J. Park, K. H. Yoon, D. S. Yoon, and T. S. Kim, Biosens. Bioelectron. **20**, 2157 (2005).
[17]R. Mukhopadhyay, V. V. Sumbayev, M. Lorentzen, J. Kjems, P. A. Andreasen, and F. Besenbacher, Nano Lett. **5**, 2385 (2005).
[18]Y. Arntz, J. D. Seelig, H. P. Lang, J. Zhang, P. Hunziker, J. P. Ramseyer, E. Meyer, M. Hegner, and C. Gerber, Nanotechnology **14**, 86 (2002).
[19]G. A. Campbell, M. B. Medina, and R. Mutharasan, Sens. Actuators, B **126**, 354 (2007).
[20]T. Braun, N. Backmann, M. Vögtli, A. Bietsch, A. Engel, H.-P. Lang, C. Gerber, and M. Hegner, Biophys. J. **90**, 2970 (2006).
[21]N. Maloney, G. Lukacs, J. Jensen, and M. Hegner, Nanoscale **6**, 8242 (2014).
[22]L. Johnson, A. K. Gupta, A. Ghafoor, D. Akin, and R. Bashir, Sens. Actuators, B **115**, 189 (2006).
[23]R. Berger, E. Delamarche, H. P. Lang, C. Gerber, J. K. Gimzewski, and E. Meyer, Science **276**, 2021 (1997).
[24]M. Godin, V. Tabard-Cossa, Y. Miyahara, T. Monga, P. J. Williams, L. Y. Beaulieu, R. Bruce Lennox, and P. Grutter, Nanotechnology **21**, 75501 (2010).
[25]G. Y. Chen, T. Thundat, E. A. Wachter, and R. J. Warmack, J. Appl. Phys. **77**, 3618 (1995).
[26]D. Ramos, J. Tamayo, J. Mertens, M. Calleja, and A. Zaballos, J. Appl. Phys. **100**, 2004 (2006).
[27]S. Sang, Y. Zhao, W. Zhang, P. Li, J. Hu, and G. Li, Biosens. Bioelectron. **51**, 124 (2014).
[28]Y.-L. Yang, M.-C. Chuang, S.-L. Lou, and J. Wang, Analyst **135**, 1230 (2010).
[29]A. Gupta, D. Akin, and R. Bashir, Appl. Phys. Lett. **84**, 1976 (2004).
[30]K. Park, L. J. Millet, N. Kim, H. Li, X. Jin, G. Popescu, N. R. Aluru, K. J. Hsia, and R. Bashir, Proc. Natl. Acad. Sci. U. S. A. **107**, 20691 (2010).
[31]K. Jensen, K. Kim, and A. Zettl, Nat. Nanotechnol. **3**, 533 (2008).
[32]W. Haiss, R. J. Nichols, K. Sass, K. P. Charle, J. K. Sass, and K. P. Charle, J. Electroanal. Chem. **452**, 199 (1998).
[33]V. Tabard-Cossa, M. Godin, I. J. Burgess, T. Monga, R. B. Lennox, and P. Grütter, Anal. Chem. **79**, 8136 (2007).
[34]H. Ibach, C. E. Bach, M. Giesen, and A. Grossmann, Surf. Sci. **375**, 107 (1997).
[35]H. Ibach, Electrochim. Acta **45**, 575 (1999).
[36]Y. Umeno, C. Elsässer, B. Meyer, P. Gumbsch, M. Nothacker, J. Weissmüller, and F. Evers, Europhys. Lett. **78**, 13001 (2007); e-print arXiv:0702441 [cond-mat].
[37]R. N. Viswanath, D. Kramer, and J. Weissmüller, Langmuir **21**, 4604 (2005).
[38]R. N. Viswanath, D. Kramer, and J. Weissmüller, Electrochim. Acta **53**, 2757 (2008).
[39]J. Weissmüller, R. N. Viswanath, D. Kramer, P. Zimmer, R. Würschum, and H. Gleiter, Science **300**, 312 (2003).
[40]C. Friesen, N. Dimitrov, R. C. Cammarata, and K. Sieradzki, Langmuir **17**, 807 (2001).
[41]Q. Deng, D.-H. Gosslar, M. Smetanin, and J. Weissmüller, Phys. Chem. Chem. Phys. **17**, 11725 (2015).
[42]Q. Deng and J. Weissmuller, Langmuir **30**, 10522 (2014).
[43]R. Morrow, D. R. McKenzie, and M. M. M. Bilek, J. Phys. D: Appl. Phys. **39**, 937 (2006).
[44]S. Trasatti and O. A. Petrii, Pure Appl. Chem. **63**, 711 (1991).
[45]A. Bard and L. Faulkner, *Electrochemical Methods - Fundamentals and Applications*, 2nd ed. (John Wiley & Sons, Inc., New York, USA, 2001).
[46]R. Morrow and D. R. McKenzie, Proc. R. Soc. A **468**, 18 (2012).
[47]R. Morrow and N. Sato, J. Phys. D: Appl. Phys. **32**, L20 (1999).
[48]G. G. Stoney, Proc. R. Soc. A **82**, 172 (1909).
[49]W. R. Fawcett, Condens. Matter Phys. **8**, 413 (2005).
[50]W. M. Haynes, in *Handbook of Chemistry and Physics*, 96th ed., edited by W. M. Haynes (Crc Press Llc, 2015), pp. 5–77.
[51]A. Vacic, J. M. Criscione, N. K. Rajan, E. Stern, T. M. Fahmy, and M. A. Reed, J. Am. Chem. Soc. **133**, 13886 (2011).